

SHORT COMMUNICATION

Functional characterization of cancer-associated Gab1 mutations

C Ortiz-Padilla¹, D Gallego-Ortega¹, BC Browne¹, F Hochgräfe¹, CE Caldon¹, RJ Lyons¹, DR Croucher¹, D Rickwood¹, CJ Ormandy^{1,5}, T Brummer^{2,3,4} and RJ Daly^{1,5}

Grb2-associated binder 1 (Gab1) is a docking protein that transduces signals from a variety of tyrosine kinases, including Met and the epidermal growth factor receptor (EGFR). Although the related protein Gab2 is strongly implicated in human cancer, a role for Gab1 has been less clear. However, a screen for gene mutations in breast cancer identified two somatic mutations in Gab1, Y83C and T387N. In this paper we describe the functional characterization of these Gab1 mutants. MCF-10A immortalized mammary epithelial cells overexpressing Gab1 Y83C and T387N exhibited a more elongated, fibroblastic phenotype compared with wild-type Gab1 controls. Expression of Gab1 or the mutants promoted epidermal growth factor (EGF)-independent proliferation in monolayer culture to a similar degree. However, in Matrigel culture, both mutants enhanced the formation of acini exhibiting an aberrant, branched morphology. In addition, expression of the mutants modestly increased Erk activation. The two mutants also enhanced branching morphogenesis in a different mammary epithelial cell line, HC11. To gain further insights into the mechanism of action of these mutations, we mapped Gab1 phosphorylation sites by mass spectrometry. This detected phosphorylation of T387 but not Y83. Cellular stimulation with EGF or hepatocyte growth factor (HGF) led to a transient, or sustained, induction of T387 phosphorylation, respectively. As T387 corresponds in position to Gab2 T391, which suppresses Gab2 signaling in a phosphorylation-dependent manner, these data support a model in which the T387N mutation abrogates negative-feedback regulation of Gab1. Interrogation of publically-available databases revealed additional cancer-associated mutations at, or in close proximity to, identified serine/threonine phosphorylation sites in other docking proteins. These data indicate that aberrant Gab1 signaling can directly contribute to breast cancer progression, and that negative feedback sites in docking proteins can be targeted by oncogenic mutations.

Oncogene advance online publication, 2 July 2012; doi:10.1038/onc.2012.271

Keywords: signal transduction; protein phosphorylation; mammary; breast cancer

Grb2-associated binder 1 (Gab1) is a member of the Gab/Daughter-of-sevenless family of docking proteins, which in mammals also includes Gab2 and Gab3.¹ Gab1 couples to a variety of receptor and non-receptor tyrosine kinases, including the epidermal growth factor receptor (EGFR), c-Met and Src, and, depending on context, elicits a variety of biological responses, including proliferation, migration and branching tubulogenesis.¹ It contains an N-terminal pleckstrin homology (PH) domain, a central region that harbors direct interaction sites for Grb2 and c-Met, and a large number of tyrosine phosphorylation sites. Recruitment of Gab1 to c-Met occurs via direct binding, and also via an indirect mechanism involving a Grb2 'bridge'.^{2,3} The latter mechanism is the only recruitment mode for other receptors such as the EGFR.³ The Gab1 PH domain binds phosphatidylinositol 3,4,5 trisphosphate, and this interaction localizes Gab1 to the plasma membrane in the vicinity of activated growth factor receptors⁴ and also to cell–cell contacts.⁵ Of note, the Gab1 PH domain is also required for Gab1 to promote branching tubulogenesis downstream of c-Met.⁵

Tyrosine phosphorylation of Gab1 leads to the recruitment of specific src homology 2 domain-containing effectors, which include the protein tyrosine phosphatase Shp2, the p85 subunit of phosphatidylinositol 3-kinase and the adaptor proteins Crk and

Nck.^{1,6} Binding of Shp2 leads to more sustained and/or increased activation of Ras/Erk signaling and is required for a variety of important biological effects downstream of Gab1, including cell proliferation, migration and epithelial morphogenesis.^{7–9} Gab1 is also subject to serine/threonine phosphorylation following growth factor stimulation, and this can have either positive or negative effects on signaling depending on the stimulus and cellular context.^{10–12} A more detailed characterization of phosphorylation-dependent negative feedback regulation has been undertaken for the closely-related Gab2, and to date four serine/threonine residues have been implicated in this process: S159, S210, T391 and S623.^{13–15} Phosphorylation of two of these, S210 and T391, promotes 14-3-3 binding and disassembly of the receptor/Gab2 signaling complex.¹⁴ Importantly, mutation of S159, or a combination of S210 and T391, confers transforming activity on Gab2,^{13,14} highlighting the potency of these negative feedback mechanisms.

The *GAB2* gene is amplified and/or overexpressed in breast, ovarian and gastric cancer, as well as in metastatic melanoma and acute myeloid leukemia.^{16–24} However, although Gab1 plays a critical role downstream of particular oncogenic kinases, such as Tpr-Met,⁷ there have been few reports of altered expression or mutation of Gab1 in human cancers. In one study, transcript

¹Cancer Research Program, Garvan Institute of Medical Research, Sydney, New South Wales, Australia; ²Centre for Biological Systems Analysis (ZBSA), Albert-Ludwigs-University of Freiburg, Freiburg, Germany; ³Institute for Biology III, Albert-Ludwigs-University of Freiburg, Freiburg, Germany; ⁴Centre for Biological Signalling Studies BIOS, Albert-Ludwigs-University of Freiburg, Freiburg, Germany and ⁵St Vincent's Hospital Clinical School, University of New South Wales, Sydney, New South Wales, Australia. Correspondence: Professor RJ Daly, Cancer Research Program, Garvan Institute of Medical Research, 384 Victoria Street, Sydney, New South Wales 2010, Australia.

E-mail: r.daly@garvan.org.au

Received 30 December 2011; revised 1 May 2012; accepted 21 May 2012

profiling detected increased Gab1 expression in Bcr-Abl-positive versus negative adult acute lymphoblastic leukemia,²⁵ whereas in a second study, Gab1 expression was associated with a particular subtype of medulloblastoma.²⁶ Furthermore, a screen for somatic mutations in breast and colorectal cancers identified two mutations in Gab1.²⁷ The first, Y83C, was detected in a primary ductal breast cancer, while the second, T387N, occurred in the breast cancer cell line HCC1954.

In order to gain an insight into the potential significance of the Gab1 Y83C and T387N mutations, we first considered their localization within Gab1 and their conservation in Gab1 orthologs and other members of the Gab family. Gab1 residue Y83 resides within the PH domain (Figure 1a). This residue is conserved in all Gab1 orthologs analyzed, except in *Danio rerio*, where it is replaced by another aromatic residue, phenylalanine. This residue

also replaces Y83 in Gab2 and Gab3. Gab1 T387 is located just downstream of the canonical Grb2-binding site. This residue is conserved in all Gab1 orthologs (Figure 1a). Moreover, it corresponds in position to Gab2 T391, a known site of negative regulation.¹⁴ However, it is not conserved in Gab3. The localization of Y83 and T387 to known or potential regulatory regions of Gab1, and their high degree of conservation throughout evolution, is consistent with important functional roles for these residues.

The occurrence of the two Gab1 mutations in breast cancers led us to choose MCF-10A immortalized human mammary epithelial cells for their functional characterization. Constructs expressing human influenza hemagglutinin (HA)-tagged Gab1, Gab1 Y83C and Gab1 T387N were generated in the bicistronic retroviral vector pMIG, which also encodes green fluorescent protein. These constructs were introduced into MCF-10A cells by retroviral

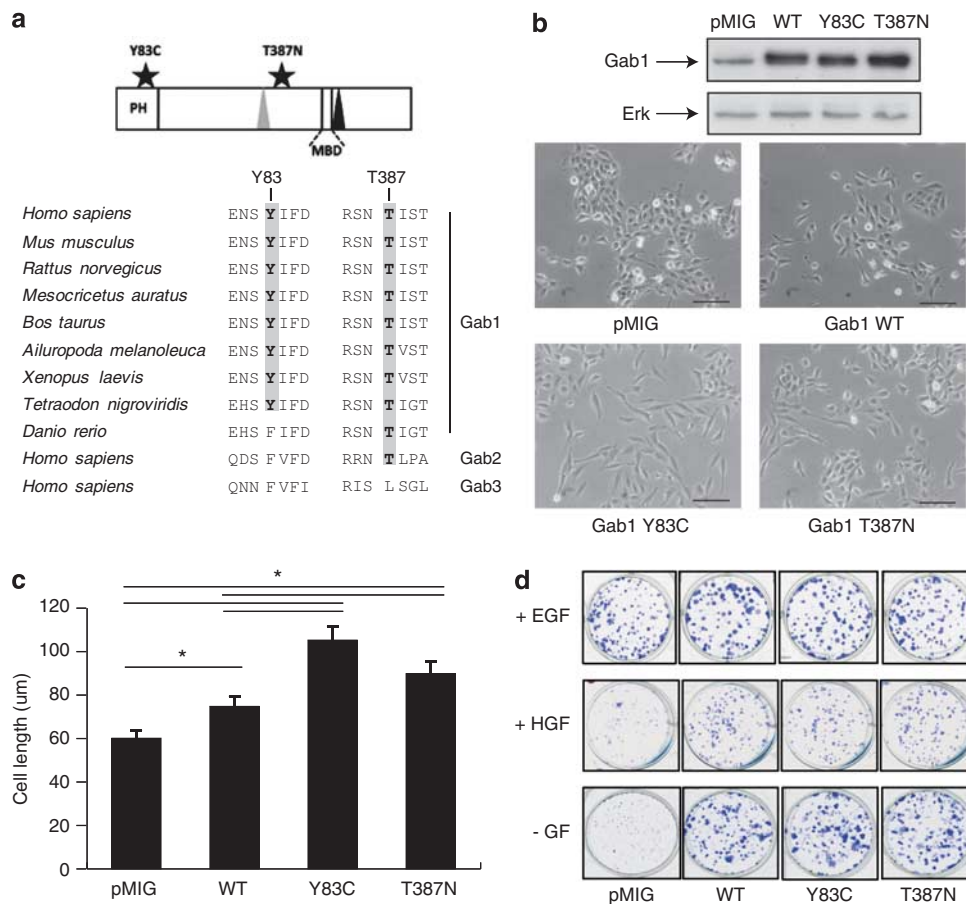


Figure 1. Characterization of cancer-associated Gab1 mutations. **(a)** Localization of Gab1 Y83 and T387 within Gab1 and sequence conservation of these residues in Gab1 orthologs and Gab2/3. The gray and black triangles indicate the canonical and non-canonical Grb2-binding sites, respectively. PH, pleckstrin homology; MBD, Met-binding domain. **(b)** Expression of Gab1 and Gab1 mutants in MCF-10A cells and resulting cellular morphology. Construction of the retroviral expression vector pMIG/Gab1-HA was as described previously.¹⁴ This used the full-length human Gab1 cDNA (splice variant isoform A, Sanger Centre IMAGE clone 303869555). The pMIG/Gab1 mutants Y83C and T387N were generated by site-directed mutagenesis (QuikChange site-directed mutagenesis Kit, Stratagene, Integrated Sciences, Willoughby, NSW, Australia). All constructs were validated by sequencing and then introduced into cells by retroviral infection, according to a published protocol.³³ Transduced cell pools were isolated by fluorescence-activated cell sorting technique. Cell lysates were prepared from monolayer and Matrigel (Becton Dickinson, North Ryde, NSW, Australia) cultures as previously described using lysis buffer containing 1% (v/v) Triton X-100 (Sigma-Aldrich, Castle Hill, NSW, Australia).³³ Western blotting was undertaken as described by Janes *et al.*⁴² Cell lysates were western blotted with antibodies against Gab1 (Millipore, Kilsyth, VIC, Australia) and total Erk (Cell Signaling Technology, Genesearch, Arundel, QLD, Australia), as indicated (top panel). The bottom panels show phase-contrast images of the isolated cell pools growing in monolayer culture. Scale bar, 200 μm. **(c)** Gab1 mutants confer a more elongate morphology. The histogram indicates cell length for each of the cell pools. Measurements of 100 cells for each pool were undertaken using Image J (NIH, <http://rsb.info.nih.gov/ij>). Error bars indicate standard error. Significance (Student's *t*-test, $P < 0.05$) is indicated using an asterisk. **(d)** Effect of Gab1 and the mutants on cell proliferation. Colony formation assays were undertaken as previously described,¹⁴ either without growth factor supplementation (– GF) or with supplementation with EGF or HGF (both 10 ng/ml). Recombinant human EGF and human cell-expressed HGF were obtained from R&D Systems (Abacus ALS, East Brisbane, QLD, Australia) and Symansis (Auckland, New Zealand), respectively.

infection, and stable pools of cells expressing similar levels of the tagged proteins were isolated by fluorescence-activated cell sorting technique (Figure 1b). In monolayer cultures, vector control cells grew as colonies with the cobblestone appearance characteristic of MCF-10A cells,²⁸ whereas cells overexpressing wild-type Gab1 were slightly elongated and exhibited reduced cell-to-cell contacts (Figure 1b). However, cells expressing Gab1 Y83C and T387N exhibited a more elongated and fibroblastic appearance (Figure 1b). Determination of cell length revealed significant increases for all Gab1-overexpressing cells compared with vector controls and, more importantly, cells expressing Gab1 mutants Y83C and T387N were significantly longer than those expressing wild-type Gab1 (Figure 1c). As these morphological changes were consistent with epithelial-mesenchymal transition (EMT), an important process during tumor progression,²⁹ we characterized the expression of several molecular markers associated with this process. This revealed that although expression of wild-type Gab1 induced changes characteristic of EMT (reduced E-cadherin expression, and enhanced levels of Twist and vimentin), these effects were not enhanced further upon expression of Gab1 Y83C or T387N (data not shown). The ability of Gab1 and the two mutants to enhance cell proliferation was determined using monolayer colony formation assays (Figure 1d). In the presence of epidermal growth factor (EGF), colony growth for all the cell pools was similar, but when EGF was substituted by hepatocyte growth factor (HGF), or EGF was omitted from the culture medium, enhancement of colony growth by Gab1 was evident, but this effect was similar to Gab1 Y83C and T387N (Figure 1d). We also isolated cell pools with approximately threefold lower expression, however this did not enable us to detect increased mitogenic effects of the mutant proteins, in either the presence or absence of growth factors (data not shown). Consequently, under the conditions of this assay, the mitogenic potential of the mutants was similar to that of wild-type Gab1.

Three-dimensional culture of MCF-10A cells in Matrigel represents an excellent model system for characterizing the activities of potential breast cancer oncogenes, as it allows analysis of a variety of biological end points, including proliferation, survival and epithelial morphogenesis.³⁰ Of note, the activity of Gab1 has not been characterized in this model. In Matrigel culture, vector control cells underwent the epithelial morphogenesis program characteristic of MCF-10A cells, forming spherical, polarized acini with a hollow lumen.³⁰ However, all Gab1-overexpressing MCF-10A cell pools displayed a combination of aberrant morphologies, which increasingly deviated from normal morphology over time (Figure 2a). In order to characterize these phenotypes further, we undertook confocal microscopy of acini that at day 20 had been immunostained with the proliferative marker Ki67, and subjected to nuclear counterstaining with TOPRO3. Vector control acini exhibited a single-cell layer surrounding a hollow lumen. In addition, they exhibited negligible levels of Ki67 staining, consistent with the proliferative suppression that occurs in late-stage cultures.³⁰ In contrast, multilobular and branching Gab1-overexpressing structures were disorganized and displayed incomplete or absent luminal clearance. In addition, a large number of Ki67-positive cells were present (Figure 2b, data for Gab1 Y83C shown). Consequently, Gab1 overexpression in this model leads to sustained proliferation and perturbs the morphogenetic program. Interestingly, the structures we observed appear quite distinct to those generated upon chronic c-Met activation in this system. In particular, although a 'branching' phenotype was prominent among Gab1-overexpressing acini, this was characterized by elaboration of multiple extensions ending in terminal lobules, rather than the tubular network elicited by c-Met in MCF-10As.³¹ We also note that one of the phenotypes we observed, multilobular, is similar to the multiacinar structures generated upon activation of erbB2 in preformed MCF-10A acini.³² A similar explanation for the multiple phenotypes we observe, and their

complexity, is that Gab1 couples to a combination of tyrosine kinases during the morphogenetic program. For example, although the multilobular phenotype may be driven primarily via erbB/Gab1 signaling, the branched structures may require additional input from other tyrosine kinases, which may include c-Met.

Acinar morphology was assessed at each time point and structures categorized into four phenotypic groups: round or normal phenotype; ruffled, for spherical acini exhibiting subtle irregularities in the outer layer; multilobular, for non-spherical acini displaying multiple distinct lobules; and branching, for the presence of duct-like protuberant structures with a terminal lobule. The phenotypic distribution of MCF-10A acini was assessed at Day 8 and Day 16 (Figure 2c). All Gab1-overexpressing pools generated acini with a marked increase in the proportion of branching phenotypes, compared with vector controls. Importantly, expression of Gab1 Y83C and T387N resulted in a significant increase in acini with a branching phenotype compared with wild-type Gab1 (Figure 2c). Although the related Gab2 promotes EGF-independent growth of MCF-10A acini,³³ none of the cell pools were able to form acini if EGF was removed from the culture medium, or replaced with HGF.

Characterization of signaling pathway activation in 3D cultures revealed that Akt phosphorylation was not affected by expression of Gab1 or the mutants (data not shown). However, there was a trend for both mutants to amplify Erk activation to a greater extent than the wild-type protein (Figure 2d). As Erk-mediated downregulation of the pro-apoptotic protein Bim impairs luminal clearance within MCF-10A acini³⁴ and coupling of Gab1 to Shp2/Erk promotes Met-induced epithelial tubulogenesis,^{9,35} amplification of this signaling pathway is likely to make an important contribution to the effects observed on acinar morphology, including the formation of branching structures. The inability of Gab1 to also increase Akt activation in 3D culture may explain why this docking protein cannot promote growth factor-independent acinar growth, unlike Gab2.³³

In order to confirm the generality of these findings, we utilized the immortalized mouse mammary epithelial cell line HC11³⁶ (Figure 3). As in MCF-10A cells, Gab1 overexpression led to acquisition of a more elongated cellular phenotype in monolayer culture, but this effect was not enhanced in cells expressing Gab1 T387N or Y83C (Figure 3b and data not shown). In terms of EMT markers, neither Gab1 nor the two mutants affected expression of Twist or vimentin, but levels of E-cadherin were markedly lower in cells expressing Gab1 Y83C compared with vector or wild-type Gab1 controls (Figure 3a). Importantly, when the cells were grown in 3D Matrigel culture,³⁷ expression of either Gab1 Y83C or T387N significantly increased the formation of branched acinar structures compared with wild-type Gab1 (Figure 3c and d), as observed in the MCF-10A model system (Figure 2c). Our ability to detect enhanced biological activity for these mutants in two independent mammary epithelial cell lines provides strong evidence that they positively impact on Gab1 function.

As Gab1 Y83 resides in the PH domain, the Y83C mutation might modulate Gab1 localization.⁵ A precedent for this is provided by the identification of an E17K mutation in the PH domain of Akt1 in human cancers.³⁸ This mutation promotes plasma membrane association of Akt1 by altering phosphoinositide binding selectivity.³⁹ Of note, Y83 resides in the $\beta 6/\beta 7$ loop of the Gab1 PH domain, in close proximity to a $\beta 6/\beta 7$ loop arginine residue that is predicted to interact with the 4-phosphate of PI(3,4,5)P3.⁴⁰ As the presence of an aromatic residue at the Y83 position is conserved throughout evolution and in Gab2 and Gab3 (Figure 1a), a non-conservative change to cysteine is likely to perturb binding of specific phosphoinositides. Therefore, we compared the localization of wild-type Gab1 and Gab1 Y83C by anti-HA staining and confocal microscopy.¹⁴ However, we were unable to detect any difference, with both proteins exhibiting

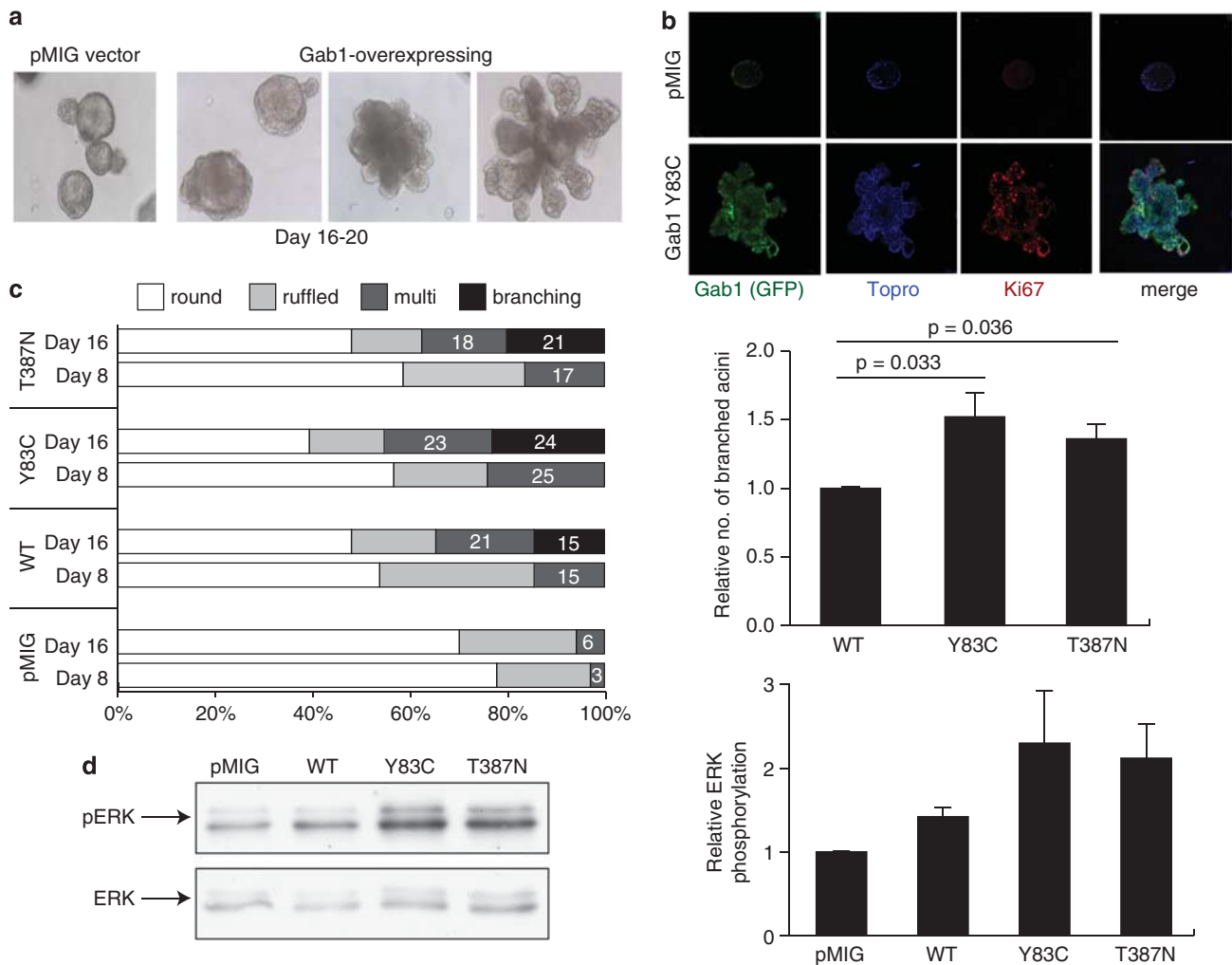


Figure 2. Effect of Gab1 and Gab1 mutants on acinar morphogenesis. **(a)** Gab1 promotes aberrant phenotypes in 3D culture. Growth of MCF-10A pools in Matrigel culture was undertaken as previously described.³³ Representative phase-contrast microscopy images ($\times 10$) of acini at days 16–20 are shown, providing examples (left to right) of round, ruffled, multilobular and branched phenotypes. **(b)** Gab1 attenuates luminal clearance and enhances proliferation within MCF-10A acini. Confocal microscopy examination of MCF-10A acini at day 20. Cells were fixed with 2% paraformaldehyde. Slides were incubated with Ki67 antibody (red) and counterstained with TOPRO3 (blue) and imaged by confocal microscopy as described previously.³³ **(c)** Quantification of phenotypic distribution for the different cell pools. Acinar morphology was assessed after 8 and 16 days of 3D culture. Phase-contrast images were taken and 80–100 acinar structures were categorized into round, ruffled, multi-lobular and branching phenotypes. The data in the left panel correspond to one representative experiment from three in total. The histogram indicates relative formation of branched acini after 16 days of culture. Data are expressed relative to the value for the wild-type Gab1 pool, which was arbitrarily set at 1.0. Data represent the mean and s.e. from three independent experiments. **(d)** Effect of Gab1 mutants on Erk activation. Cell lysates were prepared from acini after 6 days of culture as previously described³³ and western blotted for phospho and total Erk using antibodies from Cell Signaling Technology (left panel). Phosphorylated Erk was normalized for total Erk levels and then expressed relative to the value for control (vector transduced) cells, which was arbitrarily set at 1.0. In the histogram (right panel), data represent the mean and s.e. of three independent experiments.

diffuse staining throughout the cytoplasm in serum-starved cells and localizing to the plasma membrane at cell–cell junctions upon EGF or HGF stimulation (data not shown). It remains possible that Gab1 Y83C induces subtle changes in the subcellular compartmentalization of Gab1 that we were unable to detect by our imaging approach.

Next, hypothesizing that Y83 and T387 might represent novel phosphorylation sites with a negative regulatory function, we undertook a comprehensive mapping of Gab1 phosphorylation sites by LC-MS/MS. This identified nine phosphorylation sites, including T387, which represents a novel phosphoacceptor for human Gab1 (Figure 4a). Representative tandem MS spectra demonstrating T387 phosphorylation are shown in Figure 4b. Phosphorylation of Y83 was not detected. Comparison of the identified sites with the known Gab2 ‘phosphomap’^{1,14} revealed

that five of the Gab1 sites (3 serine/threonine, 2 tyrosine) are conserved in Gab2. These include T387, which corresponds to the known negative-feedback site on Gab2, T391 (Figures 1a and 4a).¹⁴

In order to characterize regulation of T387 phosphorylation, we generated a phosphospecific antibody against this site. A band corresponding to pT387 Gab1 was detected in MCF-10A cells expressing wild-type Gab1, but the intensity of this band was markedly reduced in cells expressing Gab1 T387A, confirming the selectivity of the antibody (Figure 4c). Upon stimulation of serum-starved cells with either EGF or HGF, T387 phosphorylation was increased (Figures 4c and d). However, the kinetics of T387 phosphorylation differed for the two growth factors. As shown in Figure 4d, a fourfold increase in pT387 levels was detected after 10 min of EGF stimulation. This phosphorylation level was sustained until 20 min and it then decreased, so that T387

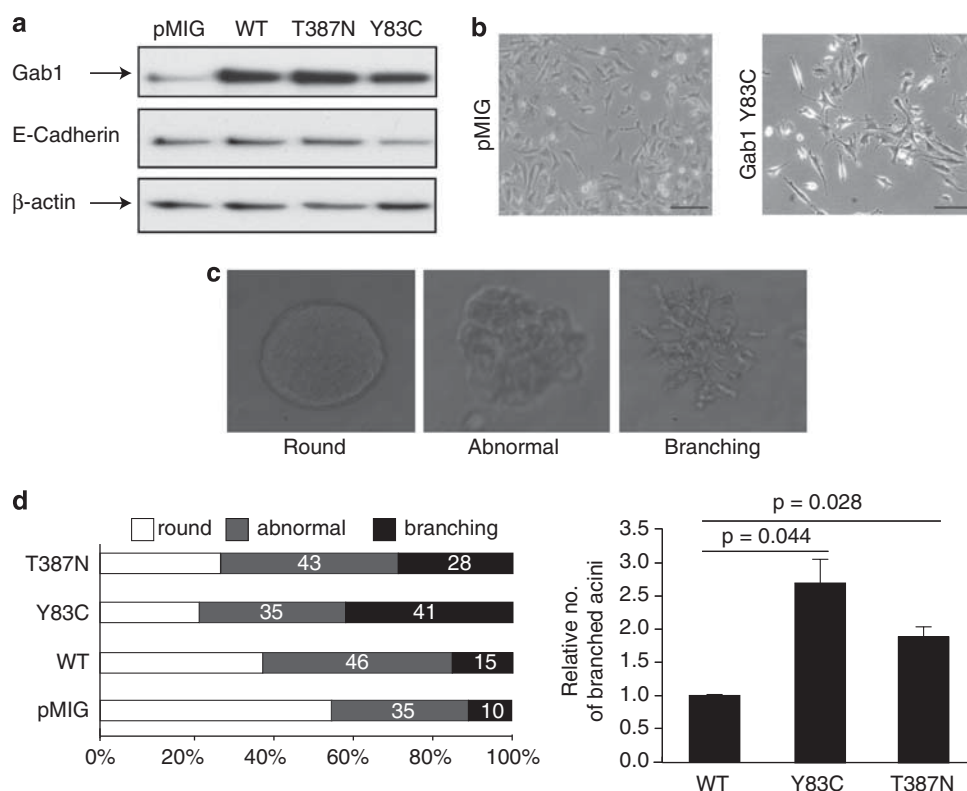


Figure 3. Functional characterization of Gab1 and the Gab1 mutants in HC11 cells. **(a)** Western blot analysis of the different cell pools. The E-cadherin and B-actin antibodies were from BD Transduction Laboratories and Sigma, respectively. **(b)** Morphology of the cell pools in monolayer culture. Scale bar, 200 μm. **(c)** Acinar morphologies displayed by the cell pools. Matrigel culture was undertaken as previously described.³⁷ Representative phase-contrast images at day 8 are shown. **(d)** Quantification of phenotypic distribution for the different cell pools. Acinar morphology was assessed after 8 days of 3D culture. Phase-contrast images were taken and 80–100 acinar structures were categorized into round, abnormal and branching phenotypes. Data are presented as in Figure 2c.

phosphorylation at 120 min of stimulation was at baseline. In contrast, phosphorylation of T387 upon HGF stimulation was slower, with the maximum signal intensity (approximately threefold above baseline) being reached at 20 min. However, it was also more sustained, being maintained above control levels (approximately twofold difference) even at 120 min of stimulation (Figure 4d). These data are consistent with Gab1 T387 acting as a site of phosphorylation-dependent negative feedback.

The identification of Gab1 T387 as a novel Gab1 phosphorylation site, its growth factor-induced phosphorylation and the biological effects of the T387N mutation indicate that this residue represents a site of negative feedback regulation. Interestingly, this site coincides in position to Gab2 T391, which resides in a consensus 14-3-3-binding motif and participates in 14-3-3-mediated negative feedback control.¹⁴ However, Gab1 T387 lacks the +2 proline characteristic of class I and II 14-3-3-binding motifs, and Gab1 is not a 14-3-3 client protein.¹⁴ This raises the question of how T387 phosphorylation regulates Gab1 signaling. One possibility is that phosphorylation of T387 induces a conformational change in Gab1 that results in similar functional consequences to phosphorylation of Gab2 T391, which promotes uncoupling of Gab2 from the receptor/Grb2 complex.¹⁴ Supporting this model is the presence of other phosphorylation sites on Gab1 that are not conserved in Gab2, and which might cooperate with T387 to induce this conformational change. A further possibility, which is not mutually exclusive with the first, is that T387 phosphorylation generates a binding site for a regulatory protein that, when bound, alters Gab1 structure.

Irrespective of the underlying mechanism, our findings demonstrate that a cancer-associated mutation can target a negative

feedback site on a docking protein. In order to determine whether additional examples of this oncogenic mechanism might exist, we undertook an integrated analysis of the COSMIC and Phosphosite databases. This identified an additional eight examples where a docking protein is mutated at, or in close proximity to, a known serine/threonine phosphorylation site (Figure 4e). We hypothesize that mutations in the vicinity of these sites could affect recognition of the phosphoacceptor residue by a particular kinase, or alter the functional consequences of phosphorylation. In the latter context, we note that a mutation in IRS-1, R1140H, alters a predicted mode I 14-3-3-binding site.⁴¹ While the functional consequences of these mutations require further characterization, the results of this analysis strongly suggest that mutation of docking proteins on negative regulatory phosphorylation sites might represent a broader phenomenon.

Expression and/or activation of several breast cancer-associated oncogenes, including erbB2 and c-Met, perturbs the morphogenetic program of MCF-10A cells in 3D culture. Consequently, the ability of the Gab1 Y83C and T387N mutations to enhance the aberrant phenotype induced by Gab1 in this system provides strong evidence that these mutations are not merely passengers but contribute to cancer progression. It also remains possible that greater functional effects may be observed in certain contexts. For example, as T387 represents a negative-feedback site, the T387N mutation may confer a stronger phenotype in the presence of certain oncogenic kinases. In the future, such information could be exploited to tailor appropriate therapies to cancer patients. For example, patients whose cancers exhibit mutations at Gab1 Y83 or T387, or equivalent regulatory sites, may respond to therapies that block signaling via the Shp2/Ras/Erk axis.

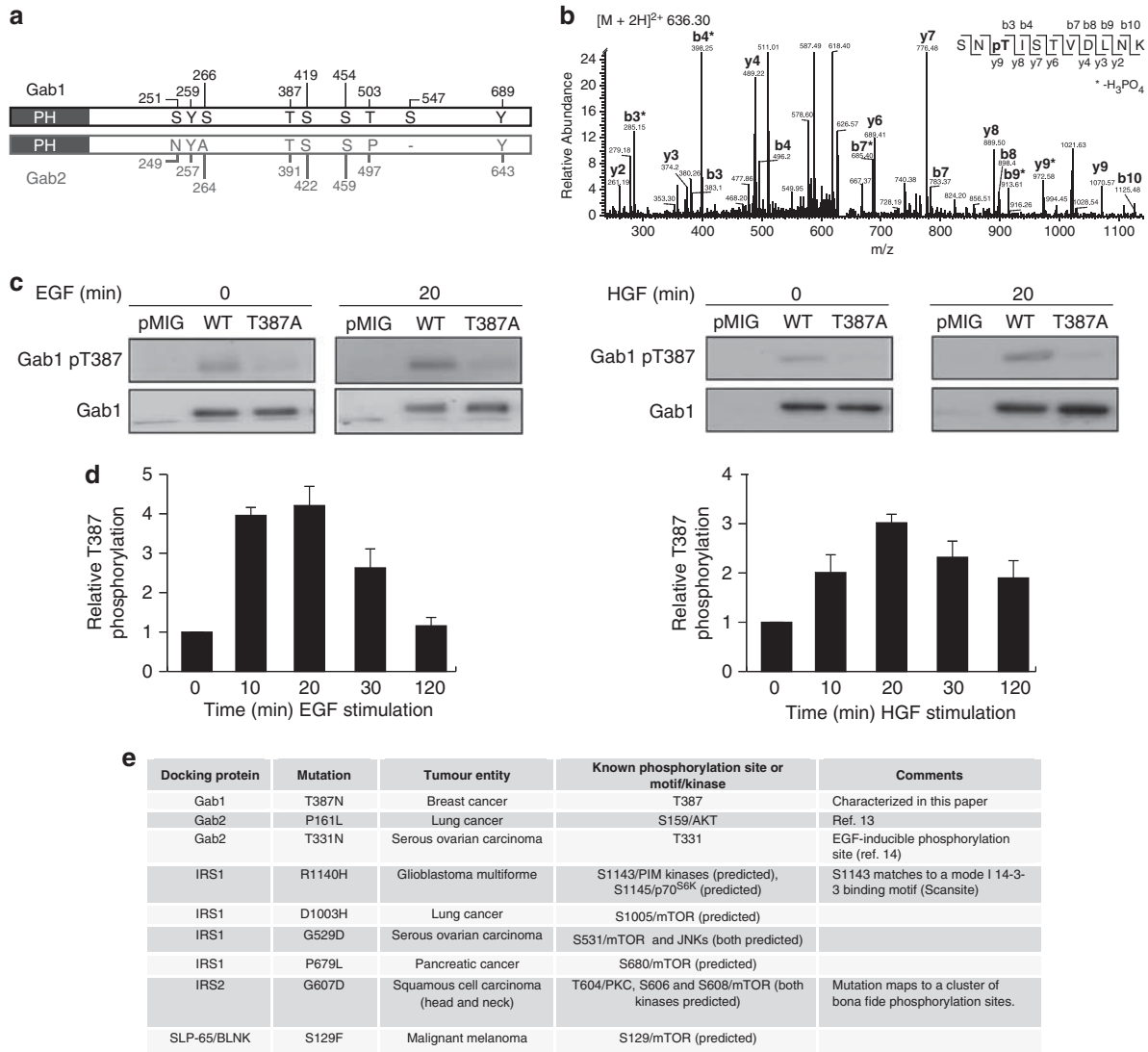


Figure 4. Negative-feedback sites on docking proteins, including Gab1 T387, can be subject to cancer-associated mutations. **(a)** Summary of phosphorylation sites identified on human Gab1 and their relationship to Gab2 phosphosites. Three 15-cm dishes of sub-confluent MCF-10A cells expressing HA-tagged Gab1 were stimulated with EGF (100 ng/ml) for 10 min. Anti-HA (clone 3F10, Roche, Castle Hill, NSW, Australia) immunoprecipitates¹⁴ were separated by SDS-PAGE and the gel stained with colloidal Coomassie. For in-gel protein digestion, gel bands of interest corresponding to the molecular weight of Gab1 were excised and prepared as previously described.¹⁴ Extracted and dried peptides were redissolved in 20 μ l of 1% formic acid (v/v), 0.05% heptafluorobutyric acid (v/v), 2% acetonitrile (v/v) and analyzed by LC-MS/MS. Briefly, peptides were separated and analyzed on an Ultimate 3000 Nano HPLC system (Dionex) directly coupled in-line with a LTQ-Orbitrap Velos mass spectrometer (Thermo Fisher Scientific). Samples were injected multiple times (5 μ l each) and measured either with or without 'multi-stage activation' option enabled and also an 'inclusion list' for fragmentation of peaks corresponding to phosphorylated and unphosphorylated peptides including amino acid 83, 317, 387, 627 or 659 of Gab1 in order to increase the probability for peptide identification. Acquired MS spectra were searched against the IPI Human database (v. 3.68) using MaxQuant (v. 1.1.1.14). Search parameters included phosphorylation of Ser/Thr/Tyr as variable modifications, maximum of two missed cleavages, 1% False Discovery Rate (FDR) filtering for site, peptide and protein identifications and a minimum peptide length of six amino acids. Additionally, phosphosites with localization probabilities > 95% were further validated by manual inspection of their tandem MS spectra. **(b)** Tandem MS spectra for the pT387-containing phosphopeptide from Gab1. **(c)** Growth factor-induced phosphorylation of Gab1 T387. Polyclonal anti-phospho-T387 antibodies were generated in sheep using standard techniques by Symansis and affinity purified on a phosphopeptide column. MCF-10A cells expressing Gab1 wild-type or T387A were serum starved and then stimulated with EGF or HGF (both 10 ng/ml) for 20 min. Cell lysates were western blotted as indicated. **(d)** Kinetics of growth factor-induced T387 phosphorylation. MCF-10A cells expressing wild-type Gab1 were stimulated with either EGF or HGF (10 ng/ml) for different times. Following western blotting, the pT387 signal was normalized for Gab1 expression. Relative Gab1 T387 phosphorylation is expressed relative to the value for serum-starved cells, which is arbitrarily set at 1.0. Data are derived from two independent experiments. Bars indicate the data range. **(e)** Somatic mutations identified in human cancers affecting known serine/threonine-phosphorylation sites or motifs in docking proteins. If not stated otherwise, somatic mutations were retrieved from the Catalog of Somatic Mutations in Cancer (COSMIC) database (<http://www.sanger.ac.uk/genetics/CGP/cosmic/>) and matched to known phosphorylation sites listed in the Phosphosite database. Phosphosite entries based on primary publications are linked to the original reference. Potential protein-protein interaction motifs and candidate kinases were predicted using the Scansite (<http://scansite.mit.edu/>) and Phosphonet (<http://www.phosphonet.ca/>) software programs, respectively. If a predicted kinase is not listed, then strong candidates were not evident from this analysis. Mutations in possible negative-feedback sites were not detected for FRS2 or DOK1-3.

CONFLICT OF INTEREST

The authors declare no conflict of interest.

ACKNOWLEDGEMENTS

This work was supported by the National Health and Medical Research Council of Australia. CEC and DRC are recipients of Cancer Institute New South Wales Early Career Fellowships. DG-O is a National Breast Cancer Foundation and Cure Cancer Australia Fellow. CJO is supported by New South Wales Cancer Council and Banque Nationale de Paris-Paribas Australia. TB is supported by the German Research Foundation (DFG) through the Emmy-Noether-Program, CRC850 and EXC294 BIOS.

REFERENCES

- Wohrle FU, Daly RJ, Brummer T. Function, regulation and pathological roles of the Gab/DOS docking proteins. *Cell Commun Signal* 2009; **7**: 22.
- Lock LS, Frigault MM, Saucier C, Park M. Grb2-independent recruitment of Gab1 requires the C-terminal lobe and structural integrity of the Met receptor kinase domain. *J Biol Chem* 2003; **278**: 30083–30090.
- Lock LS, Royal I, Naujokas MA, Park M. Identification of an atypical Grb2 carboxyl-terminal SH3 domain binding site in Gab docking proteins reveals Grb2-dependent and -independent recruitment of Gab1 to receptor tyrosine kinases. *J Biol Chem* 2000; **275**: 31536–31545.
- Rodrigues GA, Falasca M, Zhang Z, Ong SH, Schlessinger J. A novel positive feedback loop mediated by the docking protein Gab1 and phosphatidylinositol 3-kinase in epidermal growth factor receptor signaling. *Mol Cell Biol* 2000; **20**: 1448–1459.
- Maroun CR, Holgado-Madruga M, Royal I, Naujokas MA, Fournier TM, Wong AJ et al. The Gab1 PH domain is required for localization of Gab1 at sites of cell-cell contact and epithelial morphogenesis downstream from the met receptor tyrosine kinase. *Mol Cell Biol* 1999; **19**: 1784–1799.
- Abella JV, Vaillancourt R, Frigault MM, Ponzo MG, Zuo D, Sangwan V et al. The Gab1 scaffold regulates RTK-dependent dorsal ruffle formation through the adaptor Nck. *J Cell Sci* 2010; **123**: 1306–1319.
- Mood K, Saucier C, Bong YS, Lee HS, Park M, Daar IO. Gab1 is required for cell cycle transition, cell proliferation, and transformation induced by an oncogenic met receptor. *Mol Biol Cell* 2006; **17**: 3717–3728.
- Laramée M, Chabot C, Cloutier M, Stenne R, Holgado-Madruga M, Wong AJ et al. The scaffolding adapter Gab1 mediates vascular endothelial growth factor signaling and is required for endothelial cell migration and capillary formation. *J Biol Chem* 2007; **282**: 7758–7769.
- Maroun CR, Naujokas MA, Holgado-Madruga M, Wong AJ, Park M. The tyrosine phosphatase SHP-2 is required for sustained activation of extracellular signal-regulated kinase and epithelial morphogenesis downstream from the met receptor tyrosine kinase. *Mol Cell Biol* 2000; **20**: 8513–8525.
- Eulendorf R, Schaper F. A new mechanism for the regulation of Gab1 recruitment to the plasma membrane. *J Cell Sci* 2009; **122**: 55–64.
- Yu CF, Roshan B, Liu ZX, Cantley LG. ERK regulates the hepatocyte growth factor-mediated interaction of Gab1 and the phosphatidylinositol 3-kinase. *J Biol Chem* 2001; **276**: 32552–32558.
- Gual P, Giordano S, Anguissola S, Parker PJ, Comoglio PM. Gab1 phosphorylation: a novel mechanism for negative regulation of HGF receptor signaling. *Oncogene* 2001; **20**: 156–166.
- Lynch DK, Daly RJ. PKB-mediated negative feedback tightly regulates mitogenic signalling via Gab2. *EMBO J* 2002; **21**: 72–82.
- Brummer T, Larance M, Herrera Abreu MT, Lyons RJ, Timpson P, Emmerich CH et al. Phosphorylation-dependent binding of 14-3-3 terminates signalling by the Gab2 docking protein. *EMBO J* 2008; **27**: 2305–2316.
- Arnaud M, Crouin C, Deon C, Loyaux D, Bertoglio J. Phosphorylation of Grb2-associated adapter 2 on serine 623 by ERK MAPK regulates its association with the phosphatase SHP-2 and decreases STAT5 activation. *J Immunol* 2004; **173**: 3962–3971.
- Bentires-Alj M, Gil SG, Chan R, Wang ZC, Wang Y, Imanaka N et al. A role for the scaffolding adapter GAB2 in breast cancer. *Nat Med* 2006; **12**: 114–121.
- Bocanegra M, Bergamaschi A, Kim YH, Miller MA, Rajput AB, Kao J et al. Focal amplification and oncogene dependency of GAB2 in breast cancer. *Oncogene* 2010; **29**: 774–779.
- Brown LA, Kalloger SE, Miller MA, Shih le M, McKinney SE, Santos JL et al. Amplification of 11q13 in ovarian carcinoma. *Genes Chromosomes Cancer* 2008; **47**: 481–489.

- Chernoff KA, Bordone L, Horst B, Simon K, Twadell W, Lee K et al. GAB2 amplifications refine molecular classification of melanoma. *Clin Cancer Res* 2009; **15**: 4288–4291.
- Daly RJ, Gu H, Parmar J, Malaney S, Lyons RJ, Kairouz R et al. The docking protein Gab2 is overexpressed and estrogen regulated in human breast cancer. *Oncogene* 2002; **21**: 5175–5181.
- Flouren ED, O'Toole S, Millar EK, McNeil C, Lopez-Knowles E, Boulghourjian A et al. Overexpression of the oncogenic signal transducer Gab2 occurs early in breast cancer development. *Int J Cancer* 2010; **127**: 1486–1492.
- Horst B, Gruberger-Saal SK, Hopkins BD, Bordone L, Yang Y, Chernoff KA et al. Gab2-mediated signaling promotes melanoma metastasis. *Am J Pathol* 2009; **174**: 1524–1533.
- Lee SH, Jeong EG, Nam SW, Lee JY, Yoo NJ. Increased expression of Gab2, a scaffolding adaptor of the tyrosine kinase signalling, in gastric carcinomas. *Pathology* 2007; **39**: 326–329.
- Zatkova A, Schoch C, Speleman F, Poppe B, Mannhalter C, Fonatsch C et al. GAB2 is a novel target of 11q amplification in AML/MDS. *Genes Chromosomes Cancer* 2006; **45**: 798–807.
- Juric D, Lacayo NJ, Ramsey MC, Racevskis J, Wiernik PH, Rowe JM et al. Differential gene expression patterns and interaction networks in BCR-ABL-positive and -negative adult acute lymphoblastic leukemias. *J Clin Oncol* 2007; **25**: 1341–1349.
- Ellison DW, Dalton J, Kocak M, Nicholson SL, Fraga C, Neale G et al. Medulloblastoma: clinicopathological correlates of SHH, WNT, and non-SHH/WNT molecular subgroups. *Acta Neuropathol* 2011; **121**: 381–396.
- Sjoberg T, Jones S, Wood LD, Parsons DW, Lin J, Barber TD et al. The consensus coding sequences of human breast and colorectal cancers. *Science* 2006; **314**: 268–274.
- Soule HD, Maloney TM, Wolman SR, Peterson Jr WD, Brenz R, McGrath CM et al. Isolation and characterization of a spontaneously immortalized human breast epithelial cell line, MCF-10. *Cancer Res* 1990; **50**: 6075–6086.
- Drasin DJ, Robin TP, Ford HL. Breast cancer epithelial-to-mesenchymal transition: examining the functional consequences of plasticity. *Breast Cancer Res* 2011; **13**: 226.
- Debnath J, Muthuswamy SK, Brugge JS. Morphogenesis and oncogenesis of MCF-10A mammary epithelial acini grown in three-dimensional basement membrane cultures. *Methods* 2003; **30**: 256–268.
- Wrobel CN, Debnath J, Lin E, Beausoleil S, Roussel MF, Brugge JS. Autocrine CSF-1R activation promotes Src-dependent disruption of mammary epithelial architecture. *J Cell Biol* 2004; **165**: 263–273.
- Muthuswamy SK, Li D, Lelievre S, Bissell MJ, Brugge JS. ErbB2 but not ErbB1, reinitiates proliferation and induces luminal repopulation in epithelial acini. *Nat Cell Biol* 2001; **3**: 785–792.
- Brummer T, Schramek D, Hayes VM, Bennett HL, Caldon CE, Musgrove EA et al. Increased proliferation and altered growth factor dependence of human mammary epithelial cells overexpressing the Gab2 docking protein. *J Biol Chem* 2006; **281**: 626–637.
- Reginato MJ, Mills KR, Becker EB, Lynch DK, Bonni A, Muthuswamy SK et al. Bim regulation of lumen formation in cultured mammary epithelial acini is targeted by oncogenes. *Mol Cell Biol* 2005; **25**: 4591–4601.
- Khwaja A, Lehmann K, Marte BM, Downward J. Phosphoinositide 3-kinase induces scattering and tubulogenesis in epithelial cells through a novel pathway. *J Biol Chem* 1998; **273**: 18793–18801.
- Ball RK, Friis RR, Schoenenberger CA, Doppler W, Groner B. Prolactin regulation of beta-casein gene expression and of a cytosolic 120-kd protein in a cloned mouse mammary epithelial cell line. *EMBO J* 1988; **7**: 2089–2095.
- Xian W, Schwertfeger KL, Vargo-Gogola T, Rosen JM. Pleiotropic effects of FGFR1 on cell proliferation, survival, and migration in a 3D mammary epithelial cell model. *J Cell Biol* 2005; **171**: 663–673.
- Carpten JD, Faber AL, Horn C, Donoho GP, Briggs SL, Robbins CM et al. A transforming mutation in the pleckstrin homology domain of AKT1 in cancer. *Nature* 2007; **448**: 439–444.
- Landgraf KE, Pilling C, Falke JJ. Molecular mechanism of an oncogenic mutation that alters membrane targeting: Glu17Lys modifies the PIP lipid specificity of the AKT1 PH domain. *Biochemistry* 2008; **47**: 12260–12269.
- Ferguson KM, Kavran JM, Sankaran VG, Fournier E, Isakoff SJ, Skolnik EY et al. Structural basis for discrimination of 3-phosphoinositides by pleckstrin homology domains. *Mol Cell* 2000; **6**: 373–384.
- Aitken A. 14-3-3 proteins: a historic overview. *Semin Cancer Biol* 2006; **16**: 162–172.
- James PW, Daly RJ, deFazio A, Sutherland RL. Activation of the Ras signalling pathway in human breast cancer cells overexpressing erbB-2. *Oncogene* 1994; **9**: 3601–3608.